WALL-CLUTTER MITIGATION USING CROSS-BEAMFORMING IN THROUGH-THE-WALL RADAR IMAGING

Christian Debes[1], *Christian Weiss*[1], *Abdelhak M. Zoubir*[1] *and Moeness G. Amin*[2]

[1]Signal Processing Group
Technische Universität Darmstadt
Darmstadt, Germany

[2]Center for Advanced Communications
Villanova University
Villanova, PA, USA

ABSTRACT

A new technique for removal of the wall EM returns in Through-the-Wall Radar Imaging is presented. It is based on the spatial notch-filtering to separate wall and target reflections. The proposed technique forms squint beams at the receiver using a divided aperture. In doing so, it removes the strong wall signature without eliminating those of the targets. The proposed scheme provides desirable 3D target detection which is evaluated using real data examples from Through-the-Wall radar imaging experiments.

1. INTRODUCTION

In many civilian, law-enforcement and military applications it is of interest to obtain information about a scene hidden behind opaque material such as walls. This includes search-and-rescue missions and hostage crises, homeland security applications aiming at detection and classification of targets, such as humans, concealed weapons and explosives to name a few. Through-the-Wall Radar Imaging (TWRI) [1, 2] is an emerging technology, using electromagnetic wave propagation to visualize target reflections from behind walls.

It is crucial to remove the strong EM returns from the exterior wall in order to obtain radar images which reveals target location and identification. Ideally, background subtraction [3] is used in which it is assumed that empty scene measurements are available which can be coherently subtracted from measurements involving the populated scene. Background subtraction yields a significant improvement in image quality and is applicable in long-term surveillance where new targets emerge over time. Detection and classification of background-subtracted TWRI images have successfully been applied in [4, 5, 6, 7].

However, in most practical applications, it is unrealistic to assume empty or reference scene measurements being available. In these situations, wall removal techniques have to be performed using only the scene measurements at hand [8, 9, 10]. Yoon and Amin proposed a spatial filter [8] to remove wall reflections. It makes use of the fact that homogeneous wall reflections remain almost invariant across array physical or synthesized aperture, assuming it is parallel to the wall, whereas target reflections vary with antenna positions. A spatial highpass filter can, therefore, be used to suppress wall reflections.

In this paper, we propose an important extension to the wall removal technique in [8], allowing reduced clutter and noise effects in the radar images at the cost of a lower target resolution. In Section 2 and 3, we briefly review the wideband sum-and-delay beamforming technique for image formation and the wall removal technique introduced in [8]. Section 4 presents the proposed wall removal approach, followed by experimental results in Section 5. Conclusions are provided in Section 6.

2. BEAMFORMING IN THROUGH-THE-WALL RADAR IMAGING

We consider imaging a scene behind a wall using K transceivers. For simplicity, a line array is assumed. However, the concept can easily be extended to two-dimensional arrays.

The scene of interest is described by down-range/crossrange coordinates (u,v). A stepped-frequency approach [3] is considered to approximate a wideband pulse using a total of L frequencies, denoted as ω_l, $l = 0,...,L-1$. Let the received signal at the k-th antenna using the l-th frequency be denoted as the superposition of delayed target reflections,

$$z(k,\omega_l) = \sum_{p=0}^{P-1} \Gamma(u_p,v_p) e^{-j\omega_l \tau_k(u_p,v_p)} \tag{1}$$

where P is the number of point targets with $\Gamma(u_p,v_p)$ denoting the complex reflectivity of the p-th target, located at (u_p,v_p). Further, $\tau_k(u_p,v_p)$ denotes the two-way propagation delay from the k-th transceiver to the point (u_p,v_p),

$$\tau_k(u,v) = (R_{\text{air},1}(k,u,v) + \sqrt{\varepsilon} R_{\text{wall}}(k,u,v) + R_{\text{air},2}(k,u,v))/c \tag{2}$$

where ε denotes the dielectric constant of the wall and $R_{\text{air},1}(k,u,v), R_{\text{wall}}(k,u,v)$ and $R_{\text{air},2}(k,u,v)$ represent the traveling distances of the electromagnetic wave before, through and beyond the wall using the k-th antenna.

The wideband sum-and-delay beamforming for imaging is given by the summation [3]

$$I(u,v) = \sum_{l=0}^{L-1} \sum_{k=0}^{K-1} z(k,\omega_l) e^{j\omega_l \tau_k(u,v)} \tag{3}$$

3. WALL REMOVAL USING SPATIAL FILTERING

In a monostatic radar imaging approach, wall reflections are assumed to be constant along the array elements when considering a homogeneous wall, i.e. the target spatial frequency is higher than that of the wall. To remove wall reflections, a spatial filter along the line array, prior to beamforming, can be applied. As proposed in [8], we use a spatial IIR notch filter, which is advantageous if the characteristics of the wall reflections are not known exactly. It has a flexible design with a variable passband width that can be adjusted in order

 ISSN 2076-1465

to achieve desirable results, taking into account the targets' spatial frequency bandwidth. The optimal passband width depends on the target range, transmitted waveform and distance between antenna locations [8, 11].

The IIR notch filter can be described by

$$H_{NF}(\kappa) = \frac{1 - e^{-j\kappa}}{1 - \nu\, e^{-j\kappa}} \tag{4}$$

where κ is the spatial frequency and ν is the notch width. We use a two-way filtering technique, i.e., a filter in both directions of the antenna array is applied to maintain the zero phase property of the filter. Otherwise, the long impulse response of the filter would cause long target returns, which affect the target positions when performing beamforming. This would result in smearing and target defocussing effects and ghost targets may appear [8].

The first step of the wall removal technique in [8] is the spatial Fourier Transform of the received signal,

$$Z(\kappa, \omega_l) = \sum_{k=0}^{K-1} z(k, \omega_l)\, e^{-j\left(\frac{k}{K}\right)\kappa} \tag{5}$$

Applying the notch filter,

$$\widetilde{Z}(\kappa, \omega_l) \;=\; Z(\kappa, \omega_l) \;\cdot\; H_{NF}(\kappa) \tag{6}$$

results in the filtered signal for the k-th antenna element and $l = 0, \ldots, L-1$

$$\tilde{z}(k, \omega_l) = \frac{1}{K} \sum_{\kappa=0}^{K-1} \widetilde{Z}(\kappa, \omega_l)\, e^{+j\left(\frac{k}{K}\right)\kappa} \tag{7}$$

Further, applying the filter in reverse direction

$$Z_r(\kappa, \omega_l) = \sum_{k=0}^{K-1} \tilde{z}(K-1-k, \omega_l)\, e^{-j\left(\frac{k}{K}\right)\kappa} \tag{8}$$

and

$$\widetilde{Z}_r(\kappa, \omega_l) \;=\; Z_r(\kappa, \omega_l) \;\cdot\; H_{NF}(\kappa) \tag{9}$$

we obtain the two way filtered signal

$$\tilde{z}_{TW}(K-1-k, \omega_l) = \frac{1}{K} \sum_{\kappa=0}^{K-1} \widetilde{Z}_r(\kappa, \omega_l)\, e^{+j\left(\frac{\kappa}{K}\right)k} \tag{10}$$

The desired signal $\tilde{z}_{TW}(k, \omega_l)$ is obtained by simply shifting the array elements again. This procedure must then be applied for every line array of the 2D sensor aperture. The image is formed via beamforming according to Equation (3), replacing $z(k, \omega_l)$ by $\tilde{z}_{TW}(k, \omega_l)$, i.e.,

$$I_{TW}(u, v) = \sum_{l=0}^{L-1} \sum_{k=0}^{K-1} \tilde{z}_{TW}(k, \omega_l) e^{j\omega_l \tau_k(u,v)} \tag{11}$$

We consider the scenario depicted in Figure 1 (a) to demonstrate the beamforming results using the notch filter from [8]. It consists of a metal dihedral, trihedral and sphere hidden behind a concrete wall with thickness $d = 5.625$ inch and dielectric constant $\varepsilon = 7.66$. A 57×57 element planar array is synthesized with a single horn antenna. The image formation is performed by wideband sum-and-delay beamforming as presented in Section 2. Here, a stepped frequency continuous-wave signal in the range of 0.7 up to 3.1 GHz using 801 frequency steps is considered. Figure 1(b) shows a typical B-Scan without wall removal which results when focussing the upper part of the scene, where the dihedral and trihedral are present. It is evident that the image is strongly dominated by wall effects, rendering reliable target detection impossible. If empty scene measurements are available, the background subtraction technique can be applied resulting in the radar image shown in Figure 1(c). The wall effects are practically eliminated and the dihedral (dashed circle) and trihedral (solid circle) can clearly be seen.

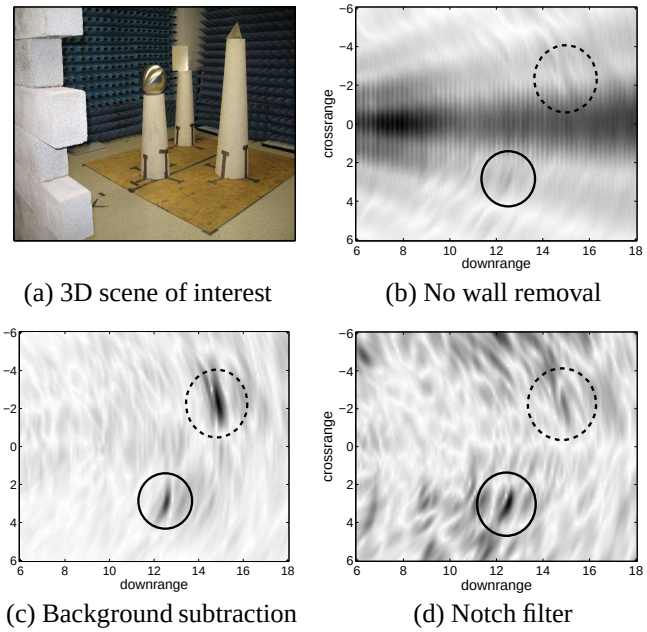

(a) 3D scene of interest (b) No wall removal

(c) Background subtraction (d) Notch filter

Figure 1: Experimental setup and acquired B-Scans

The imaging result based on the notch filter approach [8] is depicted in Figure 1(d). It is a marked improvement over Figure 1(b), but a strong amount of clutter still remains in the radar image compared with Figure 1(c). This clutter cannot be decreased by choosing a smaller filter design factor, because the clutter has a higher spatial frequency than some targets which would be removed as well. This becomes obvious when considering the dihedral in the upper right image corner. Although it has a larger radar cross section than the trihedral (cf. Figure 1(c)), it is nearly eliminated by the spatial notch filter. This is due to the fact that the corresponding EM returns for neighboring antennas do not change sufficiently and thus become subject to notch filtering suppression.

4. WALL REMOVAL USING CROSS-BEAMFORMING

As presented in Section 3, notch filtering offers a reasonable workaround for wall removal in lieu of using background subtraction. In the following, we present an extension to the spatial notch filter approach, reducing the amount of clutter and thus increasing detectability of targets. This, however, comes at the price of a reduced target resolution.

In typical behind the wall imaging, like the scenario discussed in the previous section, the weak target returns are caused by the sensors which are closest to the respective tar-

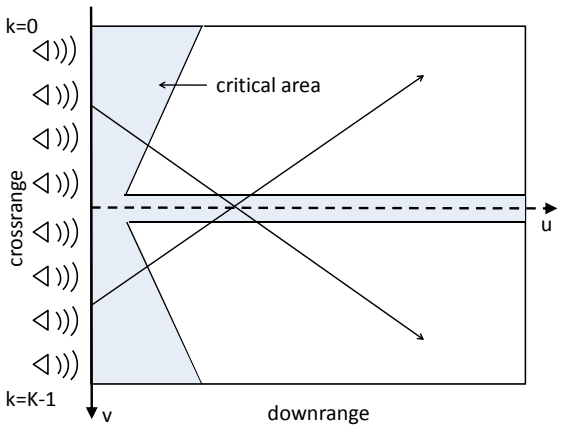

Figure 2: Example of a room segmentation and corresponding critical areas for cross-beamforming.

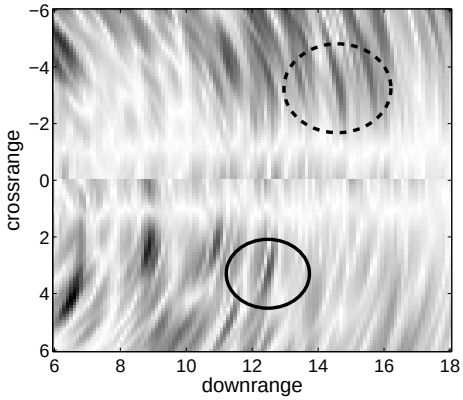

Figure 3: Imaging result when using sensors on the same side

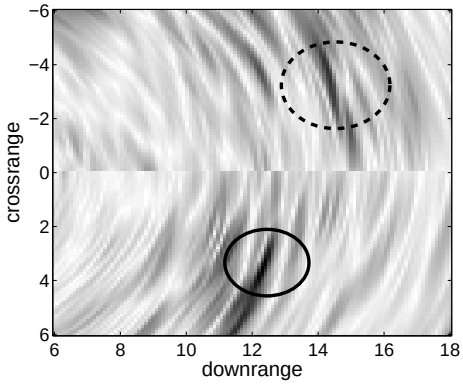

Figure 4: Imaging result when using Cross-Beamforming

get. The closer the sensors are to the target, the smaller is its spatial frequency, and consequently it is more likely that the target will be suppressed by the spatial notch filter. We propose to split the scene at the center of the sensor array and apply beamforming separately for each half of the image using only the sensors of the opposite half to encounter this problem. Figure 2 illustrates the proposed technique and highlights critical areas in the scene. The notch filtering process described by Equations (5)-(10) is also split up in two parts. Assuming an even number of sensors for simplicity, the outcomes are $\widetilde{z}_{TW,1}(k,\omega_l)$ for sensors $k = 0,...,\frac{K-1}{2}-1$ and $\widetilde{z}_{TW,2}(k,\omega_l)$ for sensors $k = \frac{K-1}{2},...,K-1$. The whole return signal is filtered as discussed in Section 3, but only the return signals of the opposite side are taken into account for beamforming. Thus, the image formation is given by

$$I(u,v) = \begin{cases} \sum_{k=0}^{\frac{K-1}{2}-1} \sum_{l=0}^{L-1} \widetilde{z}_{TW,1}(k,\omega_l) e^{-j\omega_l \tau_k(u,v)} & \text{for} \quad v > 0 \\ \sum_{k=\frac{K-1}{2}}^{K-1} \sum_{l=0}^{L-1} \widetilde{z}_{TW,2}(k,\omega_l) e^{-j\omega_l \tau_k(u,v)} & \text{for} \quad v \leq 0 \end{cases}$$

In order to verify the initial assumption that strong clutter is mainly due to sensors on the same side as the target, cross-beamforming is applied by illuminating each half of the scene using only the transceivers located on the same side. Figure 3 demonstrates that in this case, no target can be identified while strong clutter appears. Figure 4 depicts the result when correct cross-beamforming is applied, i.e., only the transceivers at the opposite side are used for imaging. It is clear that clutter is strongly reduced and both targets are visible when comparing the proposed cross-beamforming technique as in Figure 4 to the existing notch filter approach in Figure 1(d). Further, the maximum pixel values now appear at the target rather than at clutter locations, as in Figure 1(d). However, smearing effect of targets are evident due to a loss in resolution, which may be handled by considering a sliding window approach. Further, the viewing angle from the respective array center to the target is changed, which causes small target shifts.

5. EXPERIMENTAL RESULTS

We now demonstrate 3D target detection using experimental data. The same setup as introduced in Section 3 is used, consisting of a metal dihedral, trihedral and sphere. Imaging is performed through a concrete wall using a SAR system with 57×57 elements and a bandwidth of 2.4 GHz. We compare the three wall removal methods discussed in this paper, i.e., background subtraction, spatial notch filtering, as in [8], and the proposed cross-beamforming approach.

The iterative detection approach from [5] is used to evaluate the detection results in all three cases. It is an image-domain based target detector for TWRI which does not assume knowledge of the image statistics. The false-alarm rate is fixed to 1% and we restrict ourselves to square-sized morphological structuring elements [5].

Figure 5 shows the 3D detection when using background subtraction. The trihedral, dihedral and sphere (marked by solid, dashed and dotted ellipses, respectively) can clearly be detected. Only a small amount of clutter is left at approximately -5 ft crossrange / $+6$ ft downrange.

A detection map, shown in Figure 6 is obtained when using the notch filter approach [8]. As already seen when considering the B-Scan in Figure 1(d), it is hard to discriminate targets from strong clutter, which still is present all over the radar image. The detection result can considerably be improved using the proposed cross-beamforming approach as

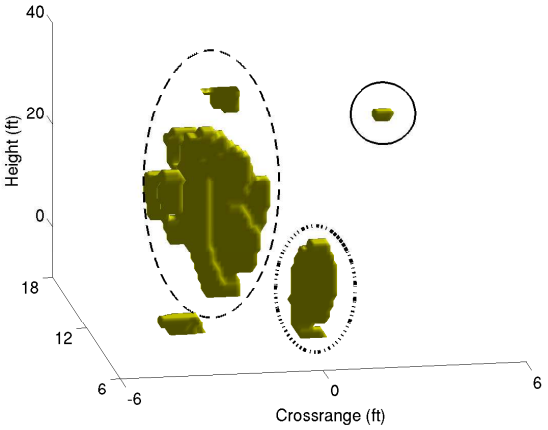

Figure 5: Detection result: Background subtraction

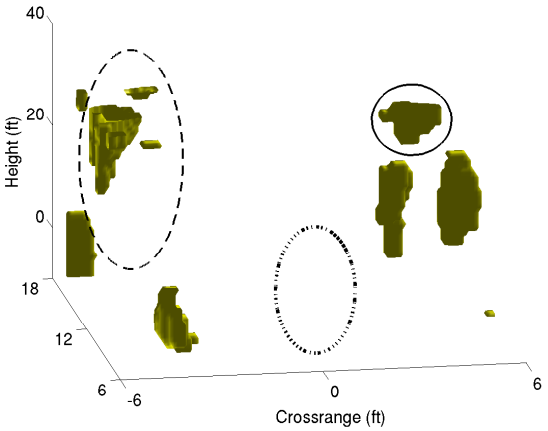

Figure 6: Detection result: Notch filter wall removal

demonstrated in Figure 7. All three targets can be detected and clutter is strongly reduced, compared to the simple notch filter approach. It should, however, be noted that the viewing angle of the respective array center to the target is also when due to the splitting of the antenna array. This ultimately yields a small displacement of the target locations [12] as evident when comparing Figures 5 and 7.

6. CONCLUSION

An effective wall-clutter mitigation using spatial notch filtering has been presented. The new approach is based on a cross-beamforming technique which splits the array aperture for imaging. Experimental data for imaging through a concrete wall was used to show a strong reduction in clutter at the cost of a reduced resolution. Automatic 3D target detection has been performed, showing the advantages of the new approach in terms of improved detection.

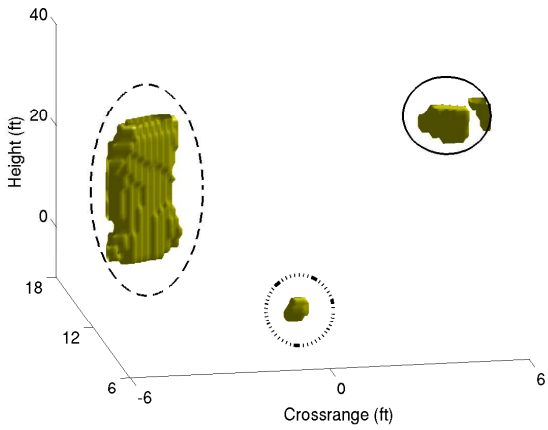

Figure 7: Detection result: Cross-Beamforming

REFERENCES

[1] M. Amin and K. Sarabandi (Guest Editors), "Special issue on remote sensing of building interior," *IEEE Transactions on Geoscience and Remote Sensing*, vol. 47, no. 5, May 2009.

[2] M. Amin (Guest Editor), "Special issue: Advances in indoor radar imaging," *Journal of the Franklin Institute*, vol. 345, no. 6, September 2008.

[3] F. Ahmad and M.G. Amin, "Multi-location wideband synthetic aperture imaging for urban sensing applications," *Journal of the Franklin Institute*, vol. 345, no. 6, pp. 618–639, Sept. 2008.

[4] C. Debes, M.G. Amin, and A.M. Zoubir, "Target detection in single- and multiple-view through-the-wall radar imaging," *IEEE Transactions on Geoscience and Remote Sensing*, vol. 47(5), pp. 1349 – 1361, May 2009.

[5] C. Debes, J. Riedler, M.G. Amin, and A.M. Zoubir, "Iterative target detection approach for through-the-wall radar imaging," in *IEEE International Conference on Acoustics, Speech and Signal Processing*, 2009, pp. 3061 – 3064.

[6] B. G. Mobasseri and Z. Rosenbaum, "3D classification of through-the-wall radar images using statistical object models," in *IEEE Workshop on Image Analysis and Interpretation*, 2008.

[7] C. Debes, J. Hahn, M.G. Amin, and A.M. Zoubir, "Feature extraction in through-the-wall radar imaging," in *IEEE International Conference on Acoustics, Speech and Signal Processing*, 2010, to appear.

[8] Y.-S. Yoon and M. G. Amin, "Spatial filtering for wall-clutter mitigation in through-the-wall radar imaging," *IEEE Transactions on Geoscience and Remote Sensing*, vol. 47, no. 9, pp. 3192–3208, 2009.

[9] M. Dehmollaian and K. Sarabandi, "Refocusing through building walls using synthetic aperture radar," *IEEE Transactions on Geoscience and Remote Sensing*, vol. 46, no. 6, pp. 1589–1599, 2008.

[10] M. Dehmollaian and K. Sarabandi, "Analytical, numerical, and experimental methods for through-the-wall radar imaging," in *IEEE International Conference on Acoustics, Speech and Signal Processing*, 2008, pp. 5181–5184.

[11] F. Gustafsson, "Determining the initial states in forward-backward filtering," *IEEE Transactions on Signal Processing*, vol. 44, no. 4, pp. 988–992, April 1996.

[12] R.J. Sullivan, *Microwave Radar Imaging and Advanced Concepts*, Artech House Inc, 2000.